CHEMISTRY
A European Journal

A Journal of
ChemPubSoc Europe

Accepted Article

Title: Formation of a cubic liquid crystalline nanostructure with π-conjugated fluorinated rods on the gyroid minimal surface

Authors: Marko Poppe, Changlon Chen, Feng Liu, Silvio Poppe, and Carsten Tschierske

To be cited as: *Chem. Eur. J.* 10.1002/chem.201700905

Link to VoR: http://dx.doi.org/10.1002/chem.201700905

Supported by
ACES

WILEY-VCH

10.1002/chem.201700905

Formation of a cubic liquid crystalline nanostructure with π-conjugated fluorinated rods on the gyroid minimal surface

Marco Poppe,[a, ‡] Changlong Chen,[b, ‡] Feng Liu,[b,*] Silvio Poppe[a] & Carsten Tschierske[a,*]

[a] M. Poppe, S. Poppe, Prof. Dr. C. Tschierske
Department of Chemistry, Martin Luther University Halle-Wittenberg, Kurt-Mothes-Str. 2, 06120 Halle, Germany
E-mail: carsten.tschierske@chemie.uni-halle.de

[b] C. Chen, Prof. Dr. F. Liu
State Key Laboratory for Mechanical Behavior of Materials,
Xi'an Jiaotong University, Xi'an 710049, P. R. China
E-mail: feng.liu@xjtu.edu.cn

‡ These authors contributed equally to this work.

Abstract: Bicontinuous cubic phases are of significant importance for numerous applications, for example, for the crystallization of membrane proteins, as photonic materials and as templates for porous silica. A new variant of bicontinuous cubic liquid crystalline phase with $Ia\bar{3}d$ lattice is reported here for X-shaped bolapolyphiles. It is shown that in this class of compounds cubic phase induction can be achieved by proper aromatic core fluorination; in addition, the first cubic phases having π-conjugated oligo(phenylene ethynylene) rods on the gyroid minimal surface were obtained. These new structures composed of 3D folded layers of parallel arranged π-conjugated rods should allow charge transport in all three dimensions, which is of interest for organic semiconductor applications.

Among nanoscale morphologies the gyroid type bicontinuous cubic phase with $Ia\bar{3}d$ space group, occurring at the transition from lamellar to columnar organization, is one of the most intriguing modes of amphiphilic self-assembly observed on different length scales in numerous systems ranging from thermotropic and lyotropic liquid crystals to block copolymer morphologies.[1,2] As shown in Figure 1c there are two interwoven networks separated by the

gyroid infinite minimal surface.[1-3] Typically the molecules forming these cubic phases are binary amphiphiles where the interfaces developing by nano-segregation of the incompatible segments assume saddle splay curvature.[4,5] Increased complexity arises if rigid linear segments are incorporated,[4] namely in rod-like molecules having bulky chains, like oligo(ethylene oxide), oligo(propylene oxide) (rod-coil molecules),[5a] siloxanes,[5b] fluorinated chains[5c-f] and long,[2a] branched[5d] or multiple alkyl chains at the ends (polycatenar molecules).[6,7] In the cubic phases of these molecules the rod-like units are organized in two interwoven networks and the flexible chains fill the spaces between them. In the networks the rods are arranged almost perpendicular to the networks with opposite helical twist between them (Figure 1a).[8]

Another kind of $Ia\bar{3}d$ phase was recently reported for rod-like T-shaped molecules with terminal glycerol groups and branched semi-perfluorinated lateral chains. In these cubic phases the rod-like units form bundles of molecules (Figure 1b) aligned with their long axes parallel to the networks.[9-11] Whatsoever in all these previously reported $Ia\bar{3}d$ phases of rod-like molecules, the gyroid minimal surface, separating the two networks, is only formed by disordered alkyl chains.

<Figure 1>

Here we report a new variant of bicontinuous $Ia\bar{3}d$ cubic structure, having π-conjugated rods organized on the gyroid minimal surface. It is obtained by fluorination of the oligo(phenylene-ethynylene) core of the X-shaped polyphile **H** (Figure 2a, all X = H) forming a triangular honeycomb liquid crystalline (LC) phase (Col_{hex} phase) in a small temperature range (Figure S11, Table S9).[12a,b] In this LC phase quasi-infinite triangular prismatic cells are formed by the packing of the aromatic cores which are fused to a triangular honeycomb by the hydrogen bonding networks of the glycerol groups at both ends, running along the edges; the lateral chains fill the interior of the honeycomb cells (Figure S12).[12-14] It is shown herein that core-fluorination[15] completely changes the mode of self-assembly, leading to bicontinuous cubic phases. In the compounds $\mathbf{F_n}$ fluorine substituents were added to the two outer benzene rings of compound **H** and the substitution pattern is identical at both ends. In the compounds names the subscripts indicate the positions of the fluorine substituents being either peripheral (directed to the glycerol units, positions 3 and 5) or directed to the core of the molecule (positions 2 and 6).

10.1002/chem.201700905

<Scheme 1, 2>

Compounds bearing one (**F$_2$**, **F$_3$**) or two fluorine atoms (**F$_{23}$**, **F$_{26}$** and **F$_{35}$**) at each end have been synthesized as shown in Scheme 1, where in a sequence of Sonogashira couplings the core unit is built up first[16] and the glycerol units are attached in one of the final steps by etherification with 1,2-isopropylidene-3-*p*-toluenesulfonyl-*rac*-glycerol. For compound **F$_{2356}$** involving two perfluorinated benzenes the synthesis starts with a nucleophilic aromatic substitution of pentafluoroiodobenzene with 1,2-isopropylideneglycerol,[17] followed by stepwise elongation of the aromatic core by successive Sonogashira couplings (Scheme 2). In both routes the deprotection of the terminal glycerol units is the final step (see supporting information).

Figure 2a shows the phase transitions on cooling for all fluorinated compounds **F$_n$** in comparison with the non-fluorinated compound **H**.[12a,b] Core fluorination reduces the melting and crystallization temperatures and widens the LC ranges (Table S1). With exception of **H** and **F$_{26}$** all compounds show optically isotropic mesophases with high viscosity, as typical for cubic phases. The structure of the cubic phases was determined by XRD with synchrotron radiation. In the WAXS region there is only diffuse scattering (Figure S10), indicating the LC nature of these cubic phases, i.e. there is no long range positional order for individual molecules. In the SAXS patterns there are series of sharp reflections with reciprocal spacings in a ratio of 1/*d*-values $6^{½}$: $8^{½}$: $20^{½}$: $22^{½}$: $24^{½}$: $26^{½}$ (Figures 3a-c and S9) which were indexed to a centred cubic lattice with space group $Ia\bar{3}d$. The cubic lattice parameters are around 9.1 nm for all compounds (Tables S2-S5). Based on the parameter the number of molecules organized in each unit cell, calculated by dividing the unit cell volume a_{cub}^3 by the molecular volume (calculated with Immirzi's crystal volume increments[18]) is almost the same, about ca 450 molecules (Table S12).

<Figure 2>

The distance between the junctions of the networks is 3.2 nm which is much shorter than the molecular length L_{mol} = 4.4 nm, measured between the ends of the glycerol groups in the most stretched conformation (Figure 2b). Even an organization with fully intercalated glycerol units would lead to a distance of 3.8 nm [(L_{mol}+L_{core})/2], still significantly exceeding the distance between the junctions. Thus, an organization in rod-bundles along the networks (Figure 1b, but having only one rod-bundle between each junction) can be excluded. The

10.1002/chem.201700905

lateral distance between the two interwoven networks is $a_{cub} \times 3^{1/2}/4 \sim 3.9$ nm (Table S12). This value is close to the layer distance in the SmA phase of compound **F$_{26}$** (d = 3.7 nm) and agrees well with the molecular length in a structure with intercalated glycerol groups, meaning that the organization of the aromatic cores is perpendicular to the gyroid minimal surface. However there are two different possibilities, either the polar glycerol groups form the networks or the minimal surface. To distinguish these possibilities electron density (ED) reconstruction was performed for the *Ia*$\bar{3}$*d* phases of compounds **F$_3$**, **F$_{35}$** and **F$_{2356}$** having different degree of fluorination. There are clear differences in the relative intensities of the reflections at larger q-values compared with the intensity of the strongest (211) scattering (Figures 3a-c and S9), indicating a changing electron density distribution. Independent on the chosen level of electron density (ED = 120, 200 respectively; note: ED is assigned from 0 to 255 after normalization for ED reconstruction, the latter one is the highest), the diameter of the high ED networks increases from **F$_2$** (blue) via **F$_{35}$** (green) to **F$_{2356}$** (red) meaning that compound **F$_{2356}$** with four fluorine at each peripheral benzene ring always has higher ED networks with larger diameter compared with its analogues compounds with lower degree of fluorination of the terminal benzene rings (Figure 3d-f). This confirms that the glycerol groups form the networks and the aromatic cores are positioned between them on the minimal surface. (Figure 1d). The area of the gyroid surface per unit cell is calculated to be about 203 nm^2,[3b] available for the ~450 molecules and meaning that the cross sectional area of each molecule is 0.4 nm^2 (see Table S12), being in line with the proposed organization of the molecules perpendicular to the minimal surfaces where the alkyl chains and aromatic cores have a similar cross sectional area of ~0.2 nm^2, agreeing well with the cross-sectional areas of these units in the LC state.[5f,19a,20] More details of ED reconstruction, phase selection and structure determination can be found in section 2.5 of the SI.

<Figure 3>

The diffuse wide angle scatterings in the cubic phases of all compounds **F$_n$** have a non-symmetric shape with a shoulder which can be fitted to a distance d = 0.32-0.35 nm (Figures 4a and S10), indicating some contribution of face-to-face π-stacking interactions between the aromatics. The shoulder is completely missing in the Col$_{hex}$ phase of **F$_2$** (see Figures 4a and S13b). Thus, it appears that π-stacking interaction develops in the *Ia*$\bar{3}$*d* cubic phase due to a restricted rotation and denser packing of the electron deficit fluorinated rings. This scattering is relatively weak and diffuse, which might be due to the limited correlation

length and the inherent saddle-splay curvature in the cubic phase. Nevertheless, it indicates that (at least local) segregation of aromatic cores and alkyl chains indeed exists. This segregation is expected to lead to triply-segregated network structures [21] or local domains in the continuum. There is first indication for such domains in the ED maps of **F$_3$** (see Figure S7d), but this requires further studies.

<Figure 4>

Analysis of the data in Figure 2a reveals that proper fluorine substitution can induce and stabilize bicontinuous cubic phases. This is remarkable, as for rod-like 4-alkoxy-4'-stilbazole complexes of silver dodecylsulfates the opposite effect was found;[6b] cubic phases of the non-fluorinated complexes were removed by peripheral fluorination and the cubic phase range was narrowed by inside directed fluorination. In contrast, all compounds **F*n*** having fluorine atoms in both peripheral positions 3 and 5 at each end (**F$_{35}$** and **F$_{2356}$**) form exclusively the cubic phases. Compounds bearing only one fluorine in the peripheral positions (**F$_3$** and **F$_{23}$**) form cubic phases, too, but on cooling a small range of a birefringent Col_{hex} is observed before the cubic phase is formed (Figure S2). However, on heating there is a direct transition Cub-Iso (Table S1), meaning that the cubic phase is the thermodynamically stable phase and the Col_{hex} phase is only metastable (therefore shown in brackets in Figure 2a). Especially remarkable is the broad cubic phase range of **F$_{2356}$** with two tetrafluorinated benzene rings, because for other rod-like[17] and polycatenar mesogens[6e] with this substitution pattern mesophase stability is known to be reduced and nematic phases were usually preferred.

Steric, polar and electronic effects of core fluorination are considered as the preliminary origins of the transition from triangular honeycombs to the cubic phases. For rod-like molecules peripheral core substitution favours smectic phases and inside directed substitution distorts layer formation, thus leading to nematic phases.[6b,19] Because the molecules **F$_n$** are arranged parallel to each other in the saddle-splay deformed layers of the *Ia*$\bar{3}$*d* phases any stabilization of smectic phases, as for example provided by core-core interactions involving the electron deficit fluorinated aromatics and electrostatic interactions, should stabilize these cubic phases, too.[15,22] However, for compounds **F$_n$** these core-core interaction could, in principle, also stabilize the organization of the aromatics along the honeycomb walls. Therefore, the situation becomes more complex and especially steric effects, depending on the position of fluorination[20] and destabilizing the honeycombs, need

to be considered. In the case of peripheral fluorination (**F_3**, **F_{35}**, **F_{23}** and **F_{2356}**) the narrow vertices in the triangular honeycombs are obviously unfavourable for this kind of self-assembly due to the clashing of the fluorine substituents (Figure 4b). Hence, fluorine substitution destabilizes the Col_{hex} phases and supports an intercalated packing of the glycerol units (Figure 4c), which reduces the interface curvature between polar and nonpolar nano-segregated regions, thus favouring the formation of the saddle-splay lamella in the $Ia\bar{3}d$ phases (Figure 4c). Figure 5 shows that replacing the peripheral fluorine of **F_3** by the larger chlorine completely removes the honeycomb, leaving only the cubic phase. Nevertheless, the larger size of Cl reduces the mesophase stability and the even larger (and non-polar) methyl group completely removes the columnar as well the cubic phase, probably by distorting the hydrogen bondings between the glycerols.

On the other hand, fluorine substituents directed towards the core region of the molecules (**F_2**, and **F_{26}**) distort the lateral core-core packing, as known for rod-like molcules where nematic phases are formed.[19] For compounds **F_n** this substitution pattern leads to the lowest LC phase stabilities and depression of the cubic phases (Figures 2, S13 and S14). Simultaneously, the disturbance of the glycerol packing in the triangular prismatic cells is reduced for **F_2**, which retains the Col_{hex} phase over a broader temperature range. For **F_{26}** the strong distortion of the core-packing by in total four of these core-directed substituents disrupts the triangular honeycomb, leading to a lamellar (SmA) phase with the lowest phase stability and fully mixed organization of alkyl chains and aromatic cores in layers (diffuse WAXS without any shoulder, see Figure S14b) separated by the polar glycerol layers. For compounds **F_{23}** and **F_{2356}**, combining peripheral with core-directed fluorination, the negative effect of core directed fluorination on cubic phase formation and mesophase stability is obviously compensated by the cubic phase stabilizing effects of the additional peripheral fluorines.

<Figure 5>

In summary, a new variant of bicontinuous cubic self-assembly with $Ia\bar{3}d$ lattice is found, which is different from, but complimentary to the organization of polycatenar mesogens by swapping the aromatic cores from the networks to the continuum. The parallel arranged π-systems on the infinite gyroid minimal surface should allow charge carrier mobility in all three dimensions of space. Though this requires further engineering of the core structure, this new type of cubic phases is of potential interest for organic semiconductor

applications, as the quasi-infinite layers of π-conjugated cores should be less sensitive to defects compared to the narrow and helical twisted networks[8] in the cubic phases of polycatenars.[23] Moreover, this work provides a blueprint for the design of 3D continuous assemblies with tethered nano-rods.[24]

Acknowledgements

This work was supported by the Deutsche Forschungsgemeinschaft (Ts 39/21-2) and the National Natural Science Foundation of China (No. 21374086). We thank beamline BL16B1 at SSRF (Shanghai Synchrotron Radiation Facility, China) for providing the beamtimes.

References

[1] a) T. Ichikawa, M. Yoshio, A. Hamasaki, S. Taguchi, F. Liu, X.-B. Zeng, G. Ungar, H. Ohno, T. Kato, *J. Am. Chem. Soc.* **2012**, *134*, 2634–2643; b) A. J. Meuler, M. A. Hillmyer, F. S. Bates, *Macromolecules* **2009**, 42, 7221-7250. c) B.-K. Cho, A. Jain, S. M. Gruner, U. Wiesner, *Science* **2004**, 305, 1598-1604; d) K. Borisch, S. Diele, P. Göring, H. Müller, C. Tschierske, *Liq. Cryst*. **1997**, *22*, 437-443.

[2] S. Kutsumizu, *Isr. J. Chem*. **2012**, *52*, 844 – 853; G. Ungar, F. Liu, X.-B. Zeng, in J. W. Goodby, J. P. Collings, T. Kato, C. Tschierske, H. F. Gleeson, P. Raynes, (Eds) Handbook of Liquid Crystals 2nd Ed. Wiley-VCH, Weinheim**, 2014**, Vol. 5, p. 363-436

[3] a) A. H. Schoen, *Interface Focus* **2012**, *2*, 658-668; b) A. H. Schoen, *NASA Technical Note TN D-5541* **1970.**

[4] C. Tschierske, *Angew. Chem. Int. Ed.* **2013**, *52*, 8828–8878.

[5] a) J.-H. Ryu, M. Lee, *Struct. Bond* **2008**, *128*, 63–98; b) E. Nishikawa, E. T. Samuslki, *Liq. Cryst*. **2000**, *27*, 1457-1462; c) M. A. Guillevic, D. W. Bruce, *Liq. Cryst*. **2000**, *27*, 153-156; d) Y. Maeda , H. Yokoyama , A. Yoshizawa, T. Kusumoto, *Liq. Cryst.* **2007**, *34*, 9–18; e) E. Nishikawa, J. Yamamoto, H. Yokoyama, *Liq. Cryst*. **2003**, *30*, 785-798; (f) C. Tschierske *Top. Curr. Chem*. **2012**, *318*, 1-108; (g) X. Cheng, M. K. Das, S. Diele, C. Tschierske, *Langmuir* **2002,** *18,* 6521-6529.

[6] a) J. Malthete, A. M. Levelut, H. L. J. Nguyen, *Phys., Lett.* **1985**, *46*, 875-880; b) D. W. Bruce, S. A. Hudson, *J. Mater. Chem*. **1994**, *4*, 479-486; c) H. L. Nguyen, C. Destrade, J. Malthete, *Adv. Mater.* **1997**, *9*, 475-388; d) D. W. Bruce, *Acc. Chem. Res*. **2000**, *33*, 831-840; e) A. I. Smirnova, B. Heinrich, B. Donnio, D. W. Bruce, *RSC Adv.* **2015**, *5*, 75149–75159; f) W. Weissflog in J. W. Goodby, J. P. Collings, T. Kato, C. Tschierske, H. F.

Gleeson, P. Raynes, (Eds) Handbook of Liquid Crystals 2nd Ed. Wiley-VCH, Weinheim, **2014**, Vol. 5, p. 89-174.#

[7] A special case of cubic phase formation is provided by rod-like 4-alkoxy-4'-stilbazole complexes of silver dodecylsulfates, having only two terminal chains and the dodecyl chains at the anion contributing to interface curvature.[6b]

[8] C. Dressel, F. Liu, M. Prehm, X.-B. Zeng, G. Ungar, C. Tschierske, *Angew. Chem. Int. Ed.* **2014,** *53*, 13115-13120.

[9] M. Prehm, F. Liu, X.-B. Zeng, G. Ungar, C. Tschierske, *J. Am. Chem. Soc*. **2011**, *133*, 4906-4916; F. Liu, M. Prehm, X-B. Zeng, G. Ungar, C. Tschierske, *Angew. Chem., Int. Ed*. **2011**, *50*, 10599-10602.

[10] F. Liu, M. Prehm, X.-B. Zeng, C. Tschierske, G. Ungar, *J. Am. Chem. Soc.* **2014**, *136*, 6846–6849.

[11] X.-B. Zeng, M. Prehm, G. Ungar, C. Tschierske, F. Liu, *Angew. Chem. Int. Ed*. **2016**, *55*, 8324-8327.

[12] a) S. Werner, H. Ebert, B.-D. Lechner, F. Lange, A. Achilles, R. Bärenwald, S. Poppe, A. Blume, K. Saalwächter, C. Tschierske, K. Bacia, *Chem. Eur. J.* **2015**, *21*, 8840–8850; b) B.-D. Lechner, H. Ebert, M. Prehm, S. Werner, A. Meister, G. Hause, A. Beerlink, K. Saalwächter, K. Bacia, C. Tschierske, A. Blume, *Langmuir* **2015**, *21*, 2839–2850; c) X. Cheng, X. Dong, G. Wie, M. Prehm, C. Tschierske, *Angew. Chem.* Angew. Chem. Int. Ed. **2009**, 48, 8014 –8017. d) X. Cheng, H. Gao, X. Tan, X. Yang, M. Prehm, H. Ebert, C. Tschierske, *Chem. Sci.* **2013**, *4*, 3317-3331.

[13] C. Tschierske, *Chem. Soc. Rev.* **2007**, *36*, 1930; S. Poppe, A. Lehmann, A. Scholte, M. Prehm, X.-B. Zeng, G. Ungar, C. Tschierske, *Nat. Commun*. **2015**, *6*, 8637.

[14] B. Glettner, F. Liu, X.-B. Zeng, M. Prehm, U. Baumeister, M. Walker, M. A. Bates, P. Boesecke, G. Ungar, C. Tschierske, *Angew. Chem. Int. Ed.* **2008**, 47, 9063–9066; X.-B. Zeng, R. Kieffer, B. Glettner, C. Nürnberger, F. Liu, K. Pelz, M. Prehm, U. Baumeister, H. Hahn, H. Lang, G.A. Gehring, C. H. M. Weber, J. K. Hobbs, C. Tschierske, G. Ungar, G. *Science* **2011**, *331*, 1302-1306; F. Liu, R. Kieffer, X.-B. Zeng, K. Pelz, M. Prehm, G. Ungar, C. Tschierske, *Nature Commun*. **2012**, *3*, 1104.

[15] K. Kishikawa, *Isr. J. Chem*. **2012,** *52*, 800 – 808; C. Dai, P. Nguyen, T. B. Marder, A. J. Scott, W. Clegg, C. Viney, *Chem. Commun.* **1999**, *24*, 2493–2494. K. B. Woody, J. E. Bullock, S. R. Parkin, M. D. Watson, *Macromolecules* **2007,** *40,* 4470-4473; S. W. Watt, C. Dai, A. J. Scott, J. M. Burke, R. L. Thomas, J. C. Collings; C. Viney, W. Clegg, T. B. Marder, *Angew. Chem. Int. Ed*. **2004**, *43*, 3061-3063.

[16] K. Sonogashira, Y. Tohda, N. Hagihara, *Tetrahedron Lett* **1975**, *50*, 4467–4470.

[17] J. Wen, M. Tian, Q. Chen, *J. Fluorine Chem.* **1994**, *68*, 117–120; Y. Xu, Y. Hu, Q. Chen, J. Wen, *J. Mater. Chem.*, **1995**, *5*, 219-221.

[18] A. Immirzi, B. Perini, *Acta Cryst. Sect. A* **1977**, *33*, 216–218.

[19] a) M. Hird, *Chem. Soc. Rev.* **2007**, *36*, 2070–2095; b) J. W. Goodby, I. M. Saez, S. J. Cowling, J. S. Gasowska, R. A. MacDonald, S. Sia, P. Watson, K. J. Toyne, M. Hird, R. A. Lewis, S.-E. Lee, V. Vaschenko, *Liq. Cryst.* **2009**, *36*, 567–605.

[20] T. A. Lobko, B. I. Ostrovskii, A. I. Pavluchenko, S. N. Sulianov, *Liq. Cryst*, **1993**, *15*, 361-376 .

[21] J. J. K. Kirkensgaard, M. E. Evans, L. de Campo, S. T. Hyde, *PNAS* **2014**, *111*, 1271–1276.

[22] C. R. Martinez, B. L. Iverson, *Chem. Sci*. **2012**, *3*, 2191–2201.

[23] T. Yasuda, H. Ooi, J. Morita, Y. Akama, K. Minoura, M. Funahashi, T. Shimomura, T. Kato, *Adv. Funct. Mater*. **2009**, 19, 411–419.

[24] (a) T. D. Nguyen, S. C. Glotzer, *ACS Nano*, **2010**, *4*, 2585-2594; (b) X. Liu, K. Yang, H. Guo, *J. Phys. Chem. B*, **2013**, *117*, 9106-9120.

Scheme and Figure captions

Scheme 1. Synthesis of $\mathbf{F_2}$, $\mathbf{F_3}$, $\mathbf{F_{23}}$, $\mathbf{F_{26}}$ and $\mathbf{F_{35}}$.[a]

[a] Reagents and conditions: i) T*i*PS-Cl, Imidazole, DCM, rt, 90 – 95%, ii) $[Pd(PPh_3)_4]$, CuI, NEt_3, reflux, 75 – 90%, iii) K_2CO_3, DCM/MeOH (2:1), rt, 35 – 65%, iv) Bu_4NF, THF, 20 °C, 80 – 90%, v) K_2CO_3, DMF, 120 °C, 24 h, 60 - 75%, vi) PPTS, THF/MeOH (1:1), 55 °C, 60 – 70%.

Scheme 2. Synthesis of $\mathbf{F_{2356}}$.[a]

[a] Reagents and conditions: i) K_2CO_3, DMF, 40 °C, 3d, 59%, ii) NEt_3, $[Pd(PPh_3)_4]$, CuI, 40 °C, 94%, iii) K_2CO_3, DCM/MeOH (2:1), 65%, iv) PPTS, MeOH/THF (1:1), 40 °C, 55%.

Figure 1. Bicontinuous cubic mesophases with $Ia\bar{3}d$ space group formed by molecules involving rod-like units (green rods): (a) polycatenar molecules;[8] (b) rod-like bolapolyphiles with branched lateral chains;[10] (c, d) the $Ia\bar{3}d$ phases of compounds $\mathbf{F_n}$: (c) reconstructed

electron density map of the cubic phase of compound **F$_{2356}$**, with the two identical infinite networks (gray) divided by the gyroid minimal surface (purple); (d) organization of the rod-like cores of the molecules on the minimal surface.

Figure 2. a) LC phases and phase transitions depending on the substitution pattern as recorded on cooling (rate 10 K min^{-1}) compounds **H**[12a,b] and **F$_n$**; abbreviations: Cr = crystalline solid, Col$_{hex}$ = hexagonal columnar LC phase (triangular honeycomb phase, for model see Figure S12); Cub/*Ia*$\bar{3}$*d* = cubic LC phase with space group *Ia*$\bar{3}$*d*; SmA = lamellar LC phase; values in brackets indicate metastable phases which can only be observed on cooling; for transitions on heating, DSC traces and transition enthalpies, see Table S1 and Figure S1; b) CPK model of compound **F$_{2356}$** with molecular dimensions.

Figure 3. a-c) SAXS diffractograms (see also Tables S2-5 and Figure S9); d, e) reconstructed electron density maps of the Cub/*Ia*$\bar{3}$*d* phases of compound **F$_{2356}$** (red), **F$_{23}$** (green) and **F$_3$** (blue) showing the isoelectron surfaces for different level of electron density (ED); f) showing the cross-sectional profile of the networks in e) using grey scale (white = high electron regions), red, green and blue represent isoelectron surfaces enclosing the high electron density regions for compound **F$_{2356}$**, **F$_{23}$** and **F$_3$** respectively, consisting of glycerol groups and fluorinated benzene rings.

Figure 4. a) Comparison of the diffuse wide angle scatterings of compound **F$_2$** in the Col$_{hex}$ phase at T = 150 °C and **F$_{23}$** in the Cub/*Ia*$\bar{3}$*d* phase at T = 160 °C (see also Figure S10); b, c) sketches showing c) the organization of the molecules in the triangular honeycombs and d) the intercalated organization of the glycerols induced by the peripheral fluorines, leading to reduced interfacial curvature and transition to Cub/*Ia*$\bar{3}$*d*; the space between the rod-like cores is filled by the lateral chains.

Figure 5. Effect of replacing fluorine (cv = 12.8 nm^3)[17] by the larger chlorine (cv = 26.7 nm^3) or a methyl group (cv = 31.7 nm^3) on the LC phases, as observed on cooling with 10 K min^{-1}; for numerical data, see Table S1.

TOC text:

10.1002/chem.201700905

The power of fluorination. Tailoring the fluorination pattern modifies the soft self-assembly of oligo(phenylene ethynylene) based X-shaped polyphiles, leading to the first thermotropic liquid crystalline cubic phase with the π-conjugated rods forming the gyroid minimal surface. The organization of the rods perpendicular to the minimal surface and parallel to each other allows π-stacking interactions in all three dimensions of space.

Keywords: liquid crystal • self-assembly • cubic phase • oligo(phenylene ethinylene) • fluorine substitution

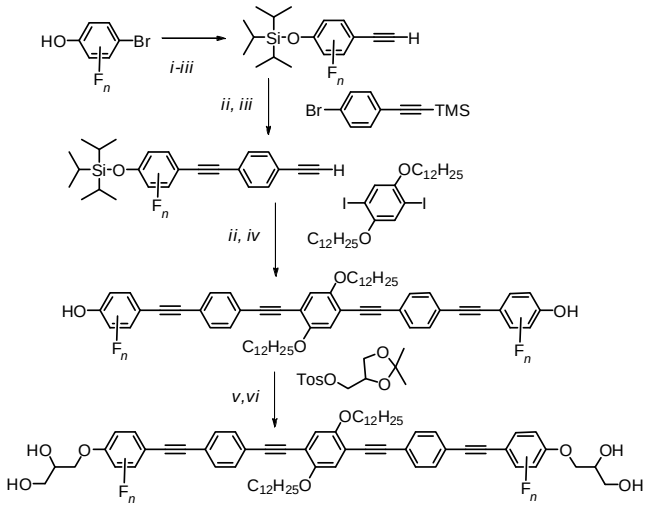

Scheme 1.

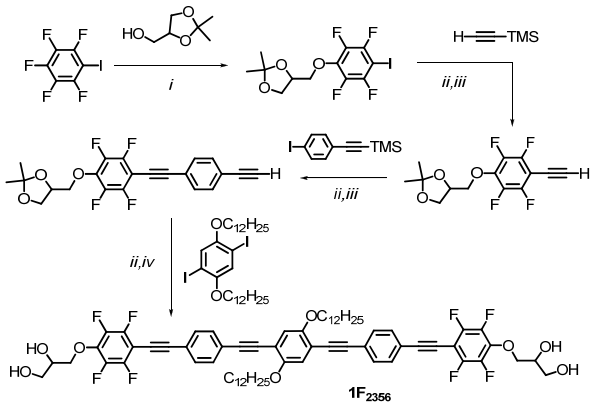

Scheme 2.

10.1002/chem.201700905

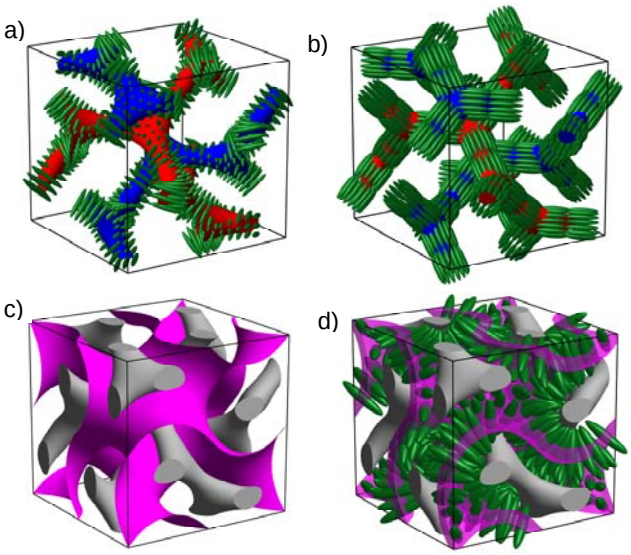

Figure 1.

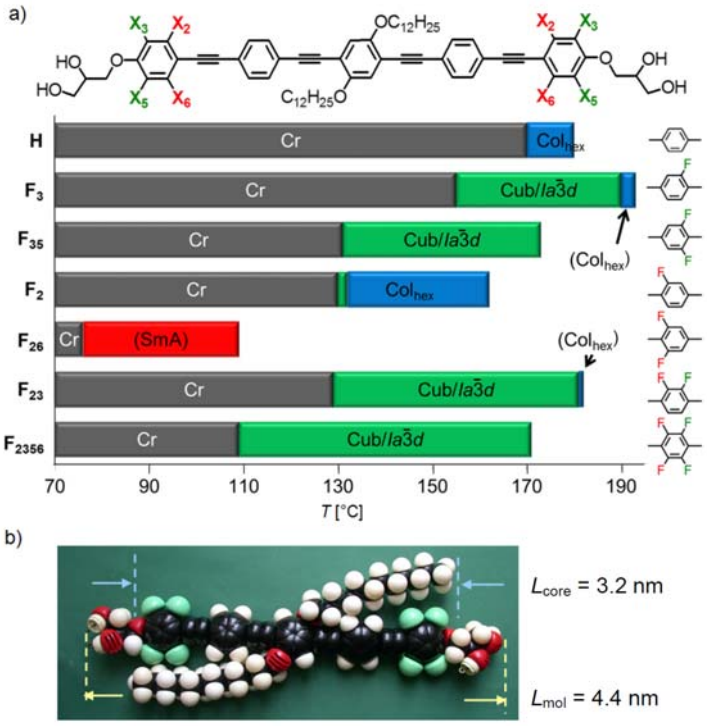

Figure 2.

10.1002/chem.201700905

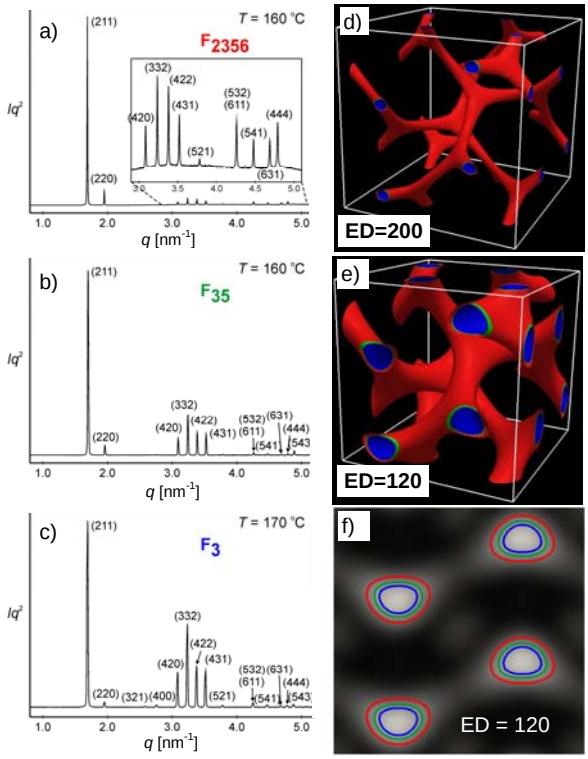

Figure 3.

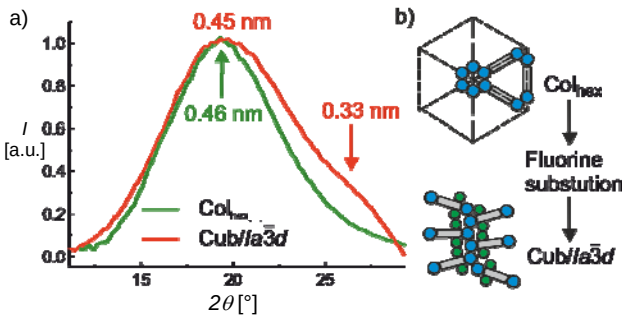

Figure 4.

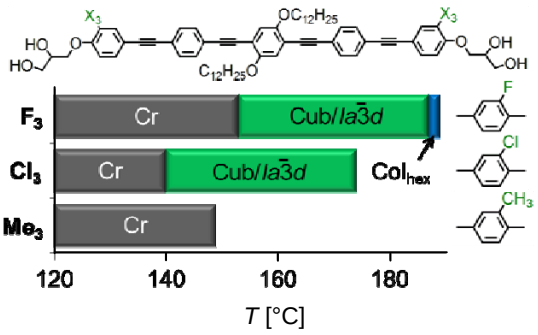

Figure 5.

10.1002/chem.201700905

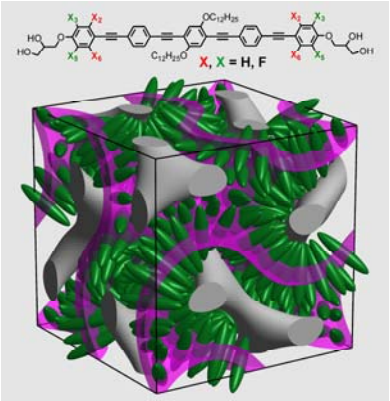

TOC Figure